Elastic Properties of Few Nanometres Thick Polycrystalline MoS 2 Membranes: A Nondestructive Study

Article *in* Nano Letters · November 2017

DOI: 10.1021/acs.nanolett.7b03669

CITATIONS
3

READS
146

7 authors, including:

Bartlomiej Graczykowski
Adam Mickiewicz University
47 PUBLICATIONS **602** CITATIONS
SEE PROFILE

Marianna Sledzinska
Catalan Institute of Nanoscience and Nanotechnology
32 PUBLICATIONS **326** CITATIONS
SEE PROFILE

Marcel Placidi
IREC Catalonia Institute for Energy Research
108 PUBLICATIONS **1,461** CITATIONS
SEE PROFILE

Maciej Kasprzak
Adam Mickiewicz University
5 PUBLICATIONS **25** CITATIONS
SEE PROFILE

Elastic Properties of Few Nanometres Thick Polycrystalline MoS_2 Membranes: A Nondestructive Study

B. Graczykowski,[*,†,‡] M. Sledzinska,[¶] M. Placidi,[§] D. Saleta Reig,[¶] M. Kasprzak,[‡,‖] F. Alzina,[¶] and C. M. Sotomayor Torres[¶,⊥]

†*Max Planck Institute for Polymer Research, Ackermannweg 10, 55128, Mainz ,Germany*
‡*NanoBioMedical Centre, Adam Mickiewicz University, Umultowska 85, 61614 Poznan, Poland*
¶*Catalan Institute of Nanoscience and Nanotechnology (ICN2), CSIC and BIST, Campus UAB, Bellaterra, 08193 Barcelona, Spain*
§*Catalonia Institute for Energy Research (IREC), Jardíns de les Dones de Negre 1, E-08930, Sant Adrià de Besòs, Spain*
‖*Faculty of Physics, Adam Mickiewicz University in Poznan, Umultowska 85, 61-614 Poznan, Poland*
⊥*ICREA, Pg. Lluís Companys 23, 08010 Barcelona, Spain*

E-mail: graczykowski@mpip-mainz.mpg.de

Abstract

The performance gain oriented nano-structurisation has opened a new pathway for tuning mechanical features of solid matter vital for application and maintained performance. Simultaneously, the mechanical evaluation has been pushed down to dimensions way below one micrometre. To date, the most standard technique to study the mechanical properties of suspended 2D materials is based on nano-indentation experiments. In this work, by means of micro-Brillouin light scattering we determine the mechanical properties, i.e. Young modulus and residual stress, of polycrystalline few nanometres thick MoS_2 membranes in a simple, contact-less, non-destructive manner. The results show huge elastic softening compared to bulk MoS_2, which is correlated with the sample morphology and the residual stress.

Keywords

Molybdenum disulfide, Elastic properties, Ultra-thin membranes, Micro-Brillouin light scattering

The translation of the remarkable electronic, mechanical, chemical, optical and thermal properties of 2D MoS_2 to potential applications relies on its mechanical properties, as these are critical for the integration into flexible and robust nano-devices and further to maintain their operational performance.[1] Undoubtedly, scaled-up fabrication of MoS_2, either by chemical vapour deposition (CVD) or Mo sulphurisation holds promise for the transfer of MoS_2 from laboratories into everyday devices.[2–6] Nevertheless, the polycrystalline morphology and residual stress of single or few-layer CVD-grown MoS_2 appear as an inevitable scenario, which can result in the change of the valuable properties expected from the single-crystalline structure.[7] On the other hand it introduces new features as band gap tuneability,[8] reduced ther-

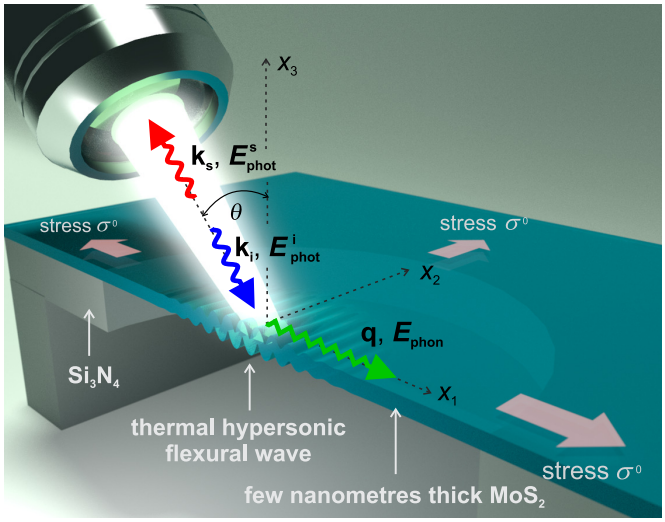

Figure 1: **Schematic illustration of micro-Brillouin backscattering geometry.** Light of $\lambda = 514.5\,\mathrm{nm}$ wave length and corresponding photon energy $E^{\mathrm{i}}_{\mathrm{phot}}$ is partially reflected from pellicle beam-splitter (R:T,8:92) and then focused on the membrane with the incident angle θ by 10×, NA = 0.25 microscope objective. The focused light spot size and power are of about few micrometres and $50\,\mu$W, respectively. The same objective acquires the scattered light of the photon energy denoted as $E^{\mathrm{s}}_{\mathrm{phot}}$, which is further cut by aperture (1 mm pinhole) and send to the tandem type Fabry-Perot spectrometer (JRS Scientific Instruments). Brillouin frequency shift doublet is defined as $\pm f = \pm E_{\mathrm{phon}}/h = (E^{\mathrm{i}}_{\mathrm{phot}} - E^{\mathrm{s}}_{\mathrm{phot}})/h$, where E_{phon} and h are acoustic phonon energy and Planck constant, respectively . The acoustic wave vector $\mathbf{q}$ is selected geometrically and of magnitude $q = 4\pi \sin\theta/\lambda$. Symbols $\mathbf{k_i}$, $\mathbf{k_s}$ denote incident light, scattered light wave vectors, respectively, and σ^0 stands for the residual biaxial stress.

mal conductivity,[9,10] enhanced photocatalitic properties[11] or high flexibility,[12] to name a few. The implementation of applications related to these features may result or require large density of grain boundaries. The mechanical properties under this condition remain experimentally unexplored as, up to now, they have been measured in single domains. To date, Young modulus and residual stress of mono and polycrystalline one- and few-layer 2D materials have been investigated by contact-like atomic force microscopy (AFM) nano-indentation[13–16] or bulge test.[17,18] However, both techniques rely on relatively large-deformations, which may result in nonlinear elastic response and induce grain boundary and dislocations dynamics effectively affecting the measurement. Furthermore, the determined values are averages taken over the whole sample, thus no spatially resolved study is possible. In this work we propose a new and straightforward approach based on micro-Brillouin light scattering (μ-BLS) within which we measure Young modulus and residual stress of large-area 5 and 10 nm thick MoS_2 membranes in nondestructive and contact-less manner.

BLS is a well-established technique for mechanical testing of bulk condensed matter. It probes light frequency shift f resulting from inelastic light scattering on thermally populated acoustic waves. Usually the probed acoustic waves are within the range of GHz frequencies (hypersound) and wavelengths of hundreds nanometres.[19,20] In our case we used tandem type Fabry-Perot interferometer and the p-p backscattering BLS geometry[19,21] (see Figure 1). The mechanical properties of the material, i.e. Young modulus E and residual stress σ^0, can be determined from the phonon dispersion $f(q)$ within the framework of the classical elastodynamics. Here, to do so we measure the dispersion of the fundamental antisymmetric (A_0) Lamb mode.[22,23]

We consider 5 and 10 nm thick membranes depicted in Figures 2a and b. The fabrication employs a polymer- and residue-free, surface-tension-assisted wet transfer of polycrystalline MoS_2, grown by means of thin Mo films sulphurisation at high temperatures from SiO_2 substrate onto circular holes made in 200 nm thick Si_3N_4 membrane.[10] The average grain size for both as-fabricated membranes is about 5 nm (see SI), what in comparison to the acoustic wave lengths measured by BLS allows the elastic continuum approximation of the membranes. Both as-fabricated membranes are uniformly flat and presumably of nonzero residual biaxial stress, which we represent by the Cauchy stress tensor $\sigma_{11} = \sigma_{22} = \sigma^0$. Interestingly, as follows from Figures 2b and c, and what we further confirm by means of μ-BLS, the 10 nm thick sample within 30 days relaxed down to visible buckling and after the same time 5 nm thick membrane remained flat. This substantial difference in ageing may be linked to a different grain orientation in these samples,

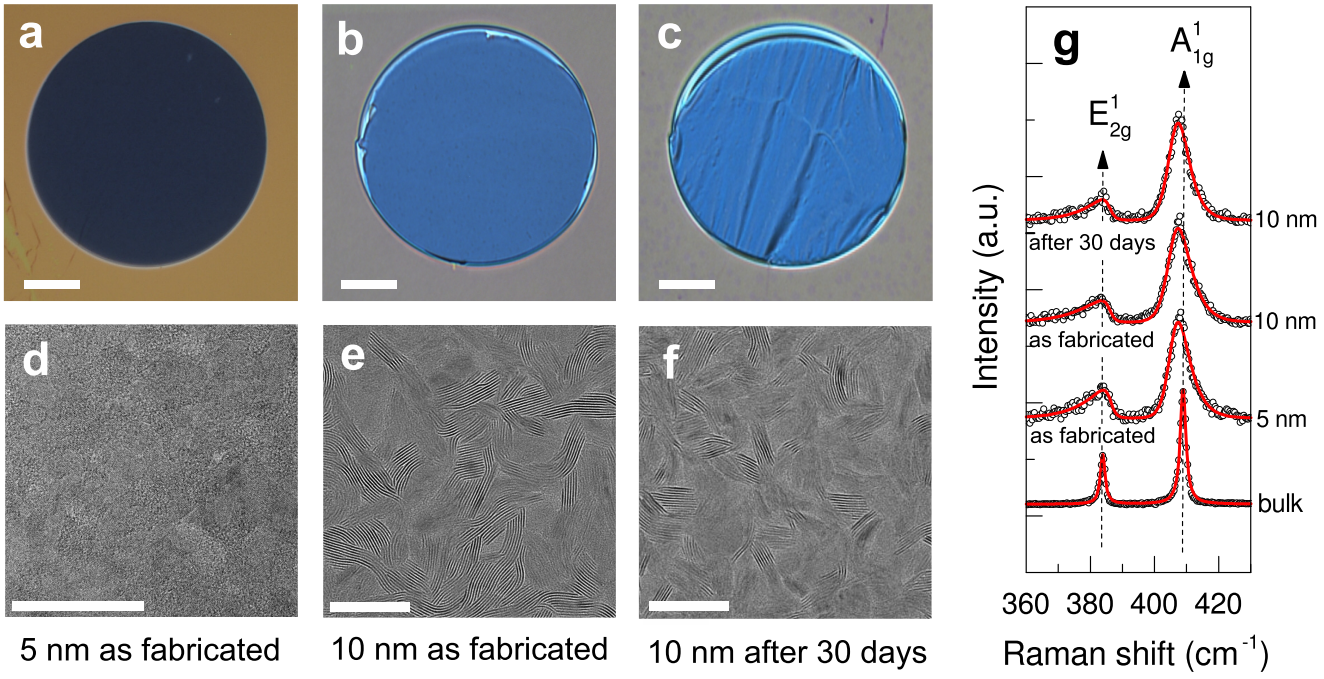

Figure 2: **MoS_2 few nanometres thick membranes.** (a-c) Optical and (d-f) transmission electron microscopy images of (a, d) 5 nm membrane, (b, e) as-fabricated and (c, f) 30 days aged 10 nm thick membranes, respectively. Membranes in (a-c) are suspended on circular holes made in 200 nm thick Si_3N_4 membrane. Scale bars in (a-c) and (d-f) are 20 μm and 5 nm, respectively. (g) Raman spectra of the membranes and bulk monocrystalline MoS_2.

which was predefined by means of the sulfurisation conditions.[24] The transmission electron microscope (TEM) image in Figure 2d shows that grains of the 5 nm thick membrane MoS_2 are aligned fully in-plane (horizontally), while for the 10 nm thick sample (Figures 2e and f) grains are of mixed orientation with van der Waals interlayer gaps exposed on the free surface. Furthermore, the grain structure is clearly manifested by Raman spectra in Figure 2g as asymmetric broadening of both E^1_{2g} and A^1_{1g} peaks.[25] These conclusions are confirmed by analysing the ratio of the integrated intensities between E^1_{2g} and A^1_{1g} modes in the Raman spectrum, which is very sensitive to the orientation of the MoS_2 layers.[24,26] While the intensity ratio of Raman modes in the 5 nm membrane is close to the value of 0.36 found in bulk MoS_2, indicating preferred horizontal orientation of the grains, both spectra of as-fabricated and relaxed 10 nm membrane show a reduced intensity ratio of 0.22. The latter corroborates the presence of mixed orientations and, since the intensity ratio remains unchanged, the preservation of the proportion of horizontally and vertically aligned grains. Interestingly, both TEM and Raman spectroscopy of 10 nm sample do not indicate any noticeable grain size or orientation change with time, which rules out them as being the origin of the residual stress reduction.

For convenience we assume full elastic isotropy for both samples. In this case polycrystalline averages of elastic constants can be estimated by the Reuss-Voigt-Hill procedure[27] (see SI). Following this and using the literature data[28] of single crystal MoS_2 we obtain the reference values, i.e. averaged Young modulus as $E_{\text{bulk}} = 104\,\text{GPa}$ and Poisson ratio to be $\nu = 0.22$. Experimental and calculated BLS spectra for example scattering angles obtained for 5 nm thick membrane are shown in Figures 3a and b, respectively. All BLS spectra of 5 nm thick sample are collected as a colourmap dispersion relation $f(q)$ in Figure 3c. For further calculations we plot the dispersion as $v_{\text{p}}(q)$ (see Figure 3d), where phase velocity is determined from $v_{\text{p}} = f\lambda/(2\sin\theta)$ and f from the Lorentzian fit of the BLS peak assigned to A_0 mode. In principle, for $q \to 0$, the dispersion $v_{\text{p}}(q)$ of A_0 for the isotropic and stretched

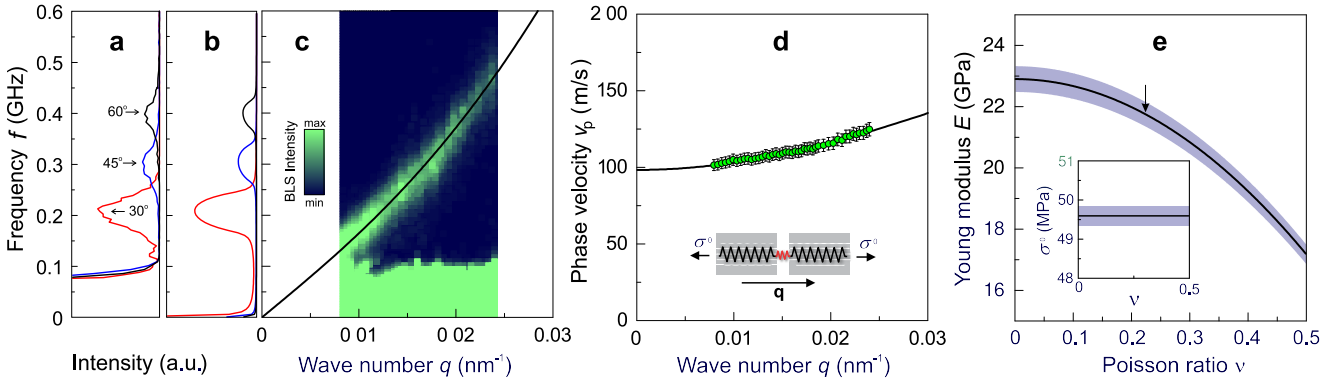

Figure 3: **Experimental results of 5 nm thick membrane.** (a) Brillouin spectra (anti-Stokes component) obtained at example scattering angles θ and (b) corresponding spectra calculated taking into account the optical and elastic properties, instrumental broadening and finite aperture of the used optics (see SI). (c) Experimental $f(q)$ dispersion relation of A_0 (colour map) and corresponding theoretical dispersion (solid line) calculated using data from Table 1. (d) Experimental (circles) and theoretical (solid line) $v_p(q)$ dispersion relations of A_0 mode. Experimental uncertainties given by Lorentzian function peaks fits are given by vertical error bars. Inset depicts schematically the relative orientation of grains, dierction of acoustic wave propagation and applied stress. (e) Calculated Young modulus and residual stress (inset) as a function of Poisson ratio. Errors are governed by the fit using Equation (1) and indicated by the shaded area. Arrow points E at ν of bulk material.

Table 1: Average grain size $\langle a \rangle$, Young modulus E and residual stress σ^0 calculated from experimental data. E is determined as an average value for ν varied form 0 to 0.5 while E' is calculated for $\nu = 0.22$. The experimental uncertainties of E includes both unspecified ν and fitting error using Equation (1), while uncertainty of E' contains only the later factor.

Sample	$\langle a \rangle$ (nm)	grain orientation	E (GPa)	E' (GPa)	σ^0 (MPa)	E_{bulk}/E'
5 nm stressed	~ 4	horizontal	20.1 ± 3.2	21.8 ± 0.5	49.6 ± 0.3	~ 5.2
10 nm stressed	~ 5	mixed	13.7 ± 2.0	14.8 ± 0.13	21.9 ± 0.2	~ 7.7
10 nm relaxed	~ 4	mixed	16.3 ± 2.1	18.1 ± 0.17	0	~ 6.3

membrane is given by (see SI):

$$v_{\text{p}} = \left[\frac{Eq^2d^2}{12\rho(1-\nu^2)} + \frac{\sigma^0}{\rho} \right]^{\frac{1}{2}}, \qquad (1)$$

where d denotes the thickness of the membrane and $\rho = 5060\,\text{kg/m}^3$ is the mass density. Equation (1) is decomposed in the way that the first, q dependent term is related to intrinsic mechanical properties, while the second, q independent term refers to the residual stress. In most of isotropic materials ν varies from 0 to 0.5, which results in a weak dependence (change of about 13%) of v_{p} on ν. Therefore, ν can be considered either as an experimental uncertainty or assumed as the same as for bulk. We note that Equation (1) remains a fair approximation if $qd <\sim 0.3$ (see SI). Otherwise, a more accurate numerical procedure is required.[21,29] The experimental dispersion in Figure 3d is clearly nonlinear and points to the presence of the residual stress. Fitting these data by means of Equation (1) we obtain E and σ^0 as a function of ν, which are plotted in Figure 3e. Here, we determine $\sigma^0 = 49.6 \pm 0.3\,\text{MPa}$ and $E = 20.1 \pm 3.2\,\text{GPa}$ for unspecified ν. Assuming bulk value of Poisson ratio, namely $\nu = 0.22$, we get $E' = 21.8 \pm 0.5\,\text{GPa}$ and corresponding in-plane and cross-plane strains as 0.18% and -0.1%, respectively. The same sample measured 30 days later did not reveal any significant change in mechanical properties (see BLS spectra in SI).

Following the same methodology we examined both as-fabricated and later relaxed 10 nm membrane. At first glance the dispersion relations $f(q)$ depicted in Figures 4a and b do not reveal any significant difference. However, the same data fitted and plotted in Figures 4c and d as $v_p(q)$ clearly indicate nonzero

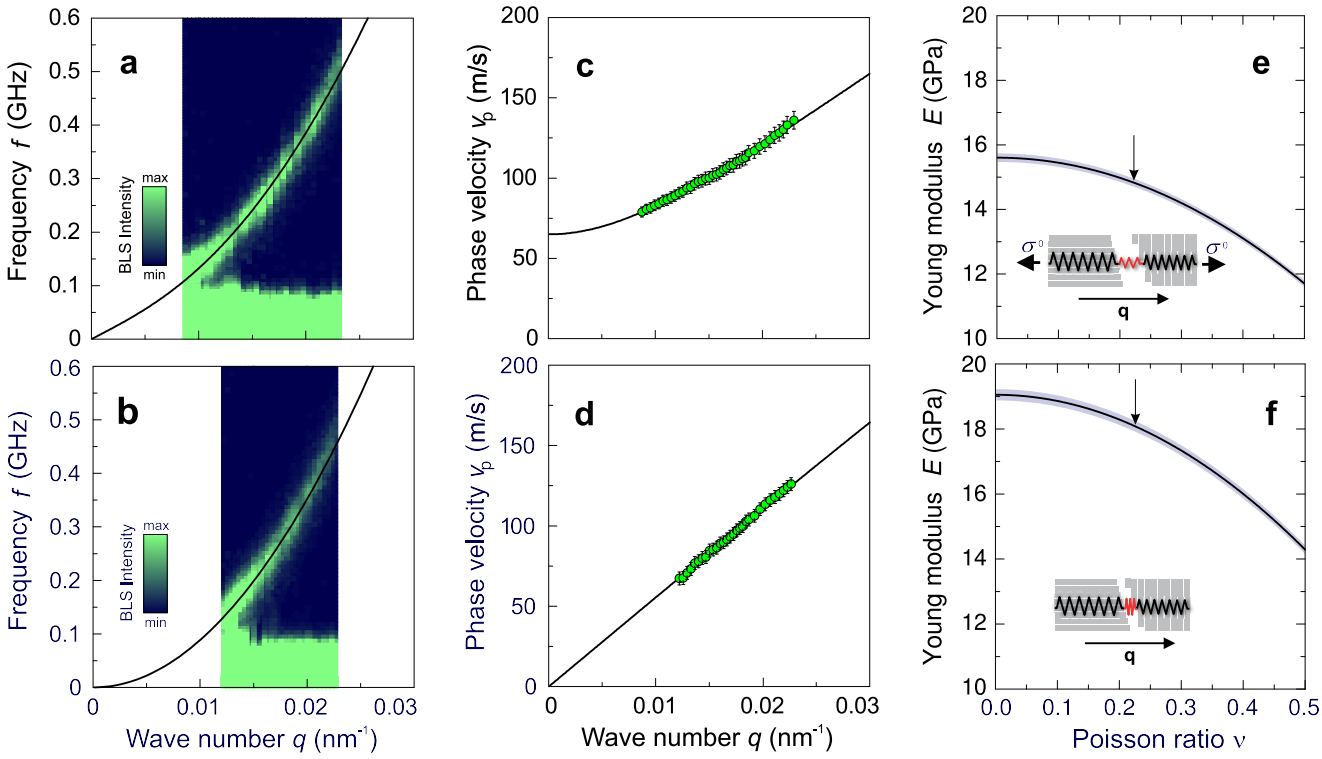

Figure 4: **Experimental results of 10 nm thick membrane.** Measured $f(q)$ dispersion relation of A_0 (colour map) and corresponding theoretical dispersion (solid line) of (a) as fabricated and (b) relaxed membrane. Experimental (circles) and theoretical (solid line) $v_p(q)$ dispersion relations of A_0 mode for (c) as fabricated and (d) relaxed membrane. Experimental uncertainties given by Lorentzian function peaks fits are given by vertical error bars. (e, f) Calculated Young modulus as a function of Poisson ratio for as fabricated and relaxed sample, respectively. Errors are governed by the fit using Equation (1) and indicated by the shaded area. Arrow points E at ν of bulk material. Insets in e and f depict schematically the relative orientation of grains, direction of acoustic wave propagation and response of the structure to the applied stress.

residual stress and its further release, respectively. For the as-fabricated sample we obtain $\sigma^0 = 21.9 \pm 0.2\,\mathrm{MPa}$, which corresponds to 0.1% in- plane and −0.06% cross-plane strains assuming $\nu = 0.22$. After 30 days, $v_p(q)$ in Figure 4d of the same sample is linear and thereby does not exhibit any stress that could be resolved by BLS. The calculated dependencies of E as a function of ν for as-fabricated and relaxed samples are plotted in Figures 4e and f, respectively.

Overall, as shown in Table 1 the measured Young moduli show strong, approximately five- to eightfold, reduction with respect to bulk polycrystalline MoS_2. Furthermore, in comparison with single crystal few-layer membranes[15] E decreases over 16-times. Following studies on metals,[30] ceramics[31] an other 2D materials[32–34] we attribute this behaviour to the small grain size and resulting high volume fraction of atoms constituting grain boundaries. In particular, both samples are of comparable grain size but of different grain orientation, what is reflected in their Young moduli and ageing. Comparing as-fabricated samples we find that 5 nm thick membrane, although thinner and upon higher stress, is about 32% stiffer than the 10 nm thick membrane. We can conclude that the predominant horizontal grain orientation in the thinner membrane ensures better grain boundary matching and/or averaging of E is done excluding weak van der Waals bonding. Going further, 5 nm membrane maintains its mechanical properties after 30 days, while 10 nm membrane relaxes the residual stress down to visible buckling and simultaneously shows distinct increase of E. We link this totally different ageing to the samples morphology, but its origin is not clear and requires more studies since, as follows from TEM and Raman

data, grain orientation and size do not change with time. Possible scenarios of the relaxation mechanism in the case of 10 nm membrane may include weaker membrane-substrate bonding and graduate slip in time or stress-driven grain boundary dynamics.[35] Noteworthy, Raman spectroscopy remains blind to that stress release (Figure 2g), although the corresponding strain would result in the redshift of E^1_{2g} mode of about $0.2 - 0.3\,\mathrm{cm}^{-1}$.[36] Thus, the material response to the applied stress seems to be inhomogeneous, i.e. the strain is distributed mostly over the dense grain boundaries, while grains remain unstrained and the determined value is an average taken over the measured area (few micrometres). This conclusion goes hand to hand with the observed increase of Young modulus in the order of GPa upon the reduction of MPa stress. Despite the corresponding strain is relatively small, typically in the regime of the linear elasticity in single crystal MoS_2,[37] the change of E proves strong nonlinear elastic behaviour that takes place at the grains boundaries.

In summary, we report on the effect of grain boundaries on the mechanical properties in polycrystalline MoS_2 membranes utilising micro-Brillouin light scattering. The proposed approach allowed an accurate assessment of Young modulus and residual stress of few nanometres thick membranes in contact-less and non-destructive way. The examined polycrystalline MoS_2 membranes showed significant elastic softening with respect to the bulk counterpart. Furthermore, we found a highly nonlinear elastic response of the sample on the stress, which we link with a non-homogenous strain distribution in the material. The presented method can be extended to any material in the form of few nanometres thick membranes.

Supporting Information.

Polycrystalline averages of elastic parameters. Phonon dispersion calculations - numerical approach. Young modulus and residual stress calculations. BLS spectra calculations. TEM diffractograms and grain distribution.

Acknowledgement ICN2 acknowledges support from the Severo Ochoa Program (MINECO, Grant SEV-2013-0295) and funding from the CERCA Programme / Generalitat de Catalunya. M.S., F.A. and C.M.S.T acknowledge the financial support from the Spanish MICINN projects PHENTOM (FIS2015-70862-P). B.G. and M.K. acknowledge the support from the Foundation for Polish Science (Homing/2016-1/2). B.G. acknowledges support from the Alexander von Humboldt foundation.

References

(1) Jariwala, D.; Sangwan, V. K.; Lauhon, L. J.; Marks, T. J.; Hersam, M. C. *ACS Nano* **2014**, *8*, 1102–1120.

(2) Lee, Y.-H.; Zhang, X.-Q.; Zhang, W.; Chang, M.-T.; Lin, C.-T.; Chang, K.-D.; Yu, Y.-C.; Wang, J. T.-W.; Chang, C.-S.; Li, L.-J.; Lin, T.-W. *Adv. Mater.* **2012**, *24*, 2320–2325.

(3) Zhan, Y.; Liu, Z.; Najmaei, S.; Ajayan, P. M.; Lou, J. *Small* **2012**, *8*, 966–971.

(4) Yu, Y.; Li, C.; Liu, Y.; Su, L.; Zhang, Y.; Cao, L. *Sci. Rep.* **2013**, *3*.

(5) Van Der Zande, A. M.; Huang, P. Y.; Chenet, D. A.; Berkelbach, T. C.; You, Y.; Lee, G.-H.; Heinz, T. F.; Reichman, D. R.; Muller, D. A.; Hone, J. C. *Nat. Mter.* **2013**, *12*, 554–561.

(6) Lloyd, D.; Liu, X.; Christopher, J. W.; Cantley, L.; Wadehra, A.; Kim, B. L.; Goldberg, B. B.; Swan, A. K.; Bunch, J. S. *Nano Letters* **2016**, *16*, 5836–5841, PMID: 27509768.

(7) Zhou, W.; Zou, X.; Najmaei, S.; Liu, Z.; Shi, Y.; Kong, J.; Lou, J.; Ajayan, P. M.; Yakobson, B. I.; Idrobo, J.-C. *Nano Lett.* **2013**, *13*, 2615–2622, PMID: 23659662.

(8) Zhang, J.; Yu, H.; Chen, W.; Tian, X.; Liu, D.; Cheng, M.; Xie, G.; Yang, W.; Yang, R.; Bai, X.; Shi, D.; Zhang, G. *ACS Nano* **2014**, *8*, 6024–6030, PMID: 24818518.

(9) Zhu, G.; Liu, J.; Zheng, Q.; Zhang, R.; Li, D.; Banerjee, D.; Cahill, D. G. *Nat. Commun.* **2016**, *7*, 13211.

(10) Sledzinska, M.; Graczykowski, B.; Placidi, M.; Reig, D. S.; El Sachat, A.; Reparaz, J.; Alzina, F.; Mortazavi, B.; Quey, R.; Colombo, L.; Roche, S.; Torres, C. S. *2D Materials* **2016**, *3*, 035016.

(11) Liu, C.; Kong, D.; Hsu, P.-C.; Yuan, H.; Lee, H.-W.; Liu, Y.; Wang, H.; Wang, S.; Yan, K.; Lin, D.; Maraccini, P. A.; Parker, K. M.; Boehm, A. B.; Cui, Y. *Nat. Nanotechnol.* **2016**, *11*, 1098–1104.

(12) Pu, J.; Yomogida, Y.; Liu, K.-K.; Li, L.-J.; Iwasa, Y.; Takenobu, T. *Nano Lett.* **2012**, *12*, 4013–4017, PMID: 22799885.

(13) Frank, I. W.; Tanenbaum, D. M.; van der Zande, A. M.; McEuen, P. L. *J. Vac. Sci. Technol., B* **2007**, *25*, 2558–2561.

(14) Poot, M.; van der Zant, H. S. J. *Appl. Phys. Lett.* **2008**, *92*, 063111.

(15) Castellanos-Gomez, A.; Poot, M.; Steele, G. A.; van der Zant, H. S. J.; Agraït, N.; Rubio-Bollinger, G. *Adv. Mater.* **2012**, *24*, 772–775.

(16) Bertolazzi, S.; Brivio, J.; Kis, A. *ACS Nano* **2011**, *5*, 9703–9709, PMID: 22087740.

(17) Vlassak, J.; Nix, W. *J. Mater. Res.* **1992**, *7*, 3242Ű3249.

(18) Turchanin, A.; Beyer, A.; Nottbohm, C. T.; Zhang, X.; Stosch, R.; Sologubenko, A.; Mayer, J.; Hinze, P.; Weimann, T.; Gölzhäuser, A. *Adv. Mater.* **2009**, *21*, 1233–1237.

(19) Speziale, S.; Marquardt, H.; Duffy, T. S. *Rev. Mineral. Geochem.* **2014**, *78*, 543–603.

(20) Schneider, D.; Gomopoulos, N.; Koh, C. Y.; Papadopoulos, P.; Kremer, F.; Thomas, E. L.; Fytas, G. *Nat. Mater.* **2016**, *15*, 1079–1083.

(21) Graczykowski, B.; Gomis-Bresco, J.; Alzina, F.; Reparaz, J.; Shchepetov, A.; Prunnila, M.; Ahopelto, J.; Torres, C. S. *New J. Phys.* **2014**, *16*, 073024.

(22) Lamb, H. *Proceedings of the Royal Society of London A: Mathematical, Physical and Engineering Sciences* **1917**, *93*, 114–128.

(23) Landau, L. D.; Lifshitz, E. M. *Theory of Elasticity*; Pergamon Press: New York, USA, 1959.

(24) Kong, D.; Wang, H.; Cha, J. J.; Pasta, M.; Koski, K. J.; Yao, J.; Cui, Y. *Nano Lett.* **2013**, *13*, 1341–1347, PMID: 23387444.

(25) Gaur, A. P. S.; Sahoo, S.; Ahmadi, M.; Guinel, M. J.-F.; Gupta, S. K.; Pandey, R.; Dey, S. K.; Katiyar, R. S. *The Journal of Physical Chemistry C* **2013**, *117*, 26262–26268.

(26) Verble, J. L.; Wieting, T. J. *Phys. Rev. Lett.* **1970**, *25*, 362–365.

(27) Hill, R. *Proc. Phys. Soc. A* **1952**, *65*, 349.

(28) Peelaers, H.; Van de Walle, C. G. *J. Phys. Chem. C* **2014**, *118*, 12073–12076.

(29) Pao, Y. H.; Sachse, W.; Fukuoka, H. *Acoustoelasticity and ultrasonic measurements of residual stress*; Physical Acoustics; Academic Press: New York, 1984; Vol. 17; pp 61–143.

(30) Schiotz, J.; Di Tolla, F. D.; Jacobsen, K. W. *Nature* **1998**, *391*, 561.

(31) Wang, Y.; Zhang, J.; Zhao, Y. *Nano Lett.* **2007**, *7*, 3196–3199, PMID: 17854230.

(32) Ruiz-Vargas, C. S.; Zhuang, H. L.; Huang, P. Y.; van der Zande, A. M.; Garg, S.; McEuen, P. L.; Muller, D. A.; Hennig, R. G.; Park, J. *Nano Lett.* **2011**, *11*, 2259–2263, PMID: 21528894.

(33) Becton, M.; Wang, X. *Phys. Chem. Chem. Phys.* **2015**, *17*, 21894–21901.

(34) Sha, Z.; Quek, S.; Pei, Q.; Liu, Z.; Wang, T.; Shenoy, V.; Zhang, Y. *Sci. Rep.* **2014**, *4*, 5991.

(35) Rupert, T.; Gianola, D.; Gan, Y.; Hemker, K. *Science* **2009**, *326*, 1686–1690.

(36) McCreary, A.; Ghosh, R.; Amani, M.; Wang, J.; Duerloo, K.-A. N.; Sharma, A.; Jarvis, K.; Reed, E. J.; Dongare, A. M.; Banerjee, S. K.; Terrones, M.; Namburu, R. R.; Dubey, M. *ACS Nano* **2016**, *10*, 3186–3197, PMID: 26881920.

(37) Cooper, R. C.; Lee, C.; Marianetti, C. A.; Wei, X.; Hone, J.; Kysar, J. W. *Phys. Rev. B* **2013**, *87*, 035423.